

Impact of flow hydrodynamics and pipe material properties on biofilm development within drinking water systems

Matthew W. Cowle , Gordon Webster , Akintunde O. Babatunde , Bettina N. Bockelmann-Evans & Andrew J. Weightman

To cite this article: Matthew W. Cowle , Gordon Webster , Akintunde O. Babatunde , Bettina N. Bockelmann-Evans & Andrew J. Weightman (2020) Impact of flow hydrodynamics and pipe material properties on biofilm development within drinking water systems, Environmental Technology, 41:28, 3732-3744, DOI: [10.1080/09593330.2019.1619844](https://doi.org/10.1080/09593330.2019.1619844)

To link to this article: <https://doi.org/10.1080/09593330.2019.1619844>



© 2019 The Author(s). Published by Informa UK Limited, trading as Taylor & Francis Group



Published online: 29 May 2019.



Submit your article to this journal [↗](#)



Article views: 1547



View related articles [↗](#)



View Crossmark data [↗](#)



Citing articles: 3 View citing articles [↗](#)

Impact of flow hydrodynamics and pipe material properties on biofilm development within drinking water systems

Matthew W. Cowle ^{a,b}, Gordon Webster ^c, Akintunde O. Babatunde^{a,d}, Bettina N. Bockelmann-Evans^a and Andrew J. Weightman ^c

^aHydro-environmental Research Centre, School of Engineering, Cardiff University, Cardiff, UK; ^bMott MacDonald, Cardiff, UK; ^cMicrobiomes, Microbes and Informatics Group, Organisms and Environment Division, School of Biosciences, Cardiff, UK; ^dInstitute of Public Health and Environmental Engineering, School of Civil Engineering, University of Leeds, Leeds, UK

ABSTRACT

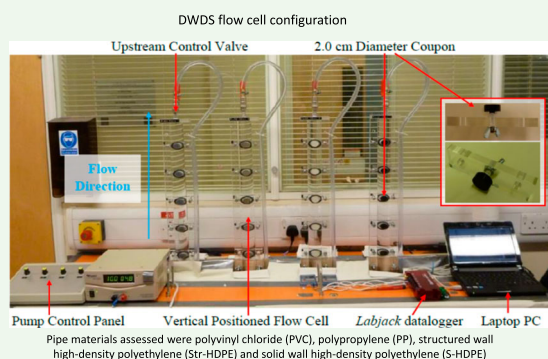
The aim of this study was to investigate the combined impact of flow hydrodynamics and pipe material on biofilm development in drinking water distribution systems (DWDS). Biofilms were formed on four commonly used pipe materials (namely polyvinyl chloride, polypropylene, structured wall high-density polyethylene and solid wall high-density polyethylene) within a series of purpose built flow cell reactors at two different flow regimes. Results indicate that varying amounts of microbial material with different morphologies were present depending on the pipe material and conditioning. The amount of microbial biomass was typically greater for the biofilms conditioned at lower flows. Whereas, biofilm development was inhibited at higher flows indicating shear forces imposed by flow conditions were above the critical levels for biofilm attachment. *Alphaproteobacteria* was the predominant bacterial group within the biofilms incubated at low flow and represented 48% of evaluated phylotypes; whilst at higher flows, *Betaproteobacteria* (45%) and *Gammaproteobacteria* (33%) were the dominant groups. The opportunistic pathogens, *Sphingomonas* and *Pseudomonas* were found to be particularly abundant in biofilms incubated at lower flows, and only found within biofilms incubated at higher flows on the rougher materials assessed. This suggests that these bacteria have limited ability to propagate within biofilms under high shear conditions without sufficient protection (roughness). These findings expand on knowledge relating to the impact of surface roughness and flow hydrodynamics on biofilm development within DWDS.

ARTICLE HISTORY

Received 20 December 2018
Accepted 7 May 2019

KEYWORDS

Biofilm; biofouling; drinking water distribution; flow hydrodynamics; pipe material



Nomenclature

h	hours	r	distance from the mean roughness height
k_{av}	mean roughness height (μm)	Re	Reynolds number
k_{rms}	root-mean-square roughness height (μm)	s_{kl}	skewness of the roughness distribution
k_s	Nikuradse-type equivalent sandgrain roughness (μm)	T	temperature ($^{\circ}\text{C}$)
k_t	maximum peak-to-trough height (μm)	\bar{U}	averaged freestream velocity (m/s)
		τ_w	wall shear stress (N/m^2)

CONTACT Matthew W. Cowle  matthew.cowle@mottmac.com  Hydro-environmental Research Centre, School of Engineering, Cardiff University, Queen's Buildings, The Parade, Cardiff, CF24 3AA, UK; Mott MacDonald, 2 Callaghan Square, Cardiff, CF10 5BT, UK; Gordon Webster  websterg@cardiff.ac.uk  Microbiomes, Microbes and Informatics Group, Organisms and Environment Division, School of Biosciences, Sir Martin Evans Building, Museum Avenue, Cardiff, CF10 3AX, UK

© 2019 The Author(s). Published by Informa UK Limited, trading as Taylor & Francis Group
This is an Open Access article distributed under the terms of the Creative Commons Attribution License (<http://creativecommons.org/licenses/by/4.0/>), which permits unrestricted use, distribution, and reproduction in any medium, provided the original work is properly cited.

1. Introduction

The prevailing environmental conditions within typical drinking water distribution systems (DWDS) are extremely adverse to bacterial life due to the inherent oligotrophic conditions, and the occasional presence of residual disinfectants. Nonetheless, bacterial based biofouling has a ubiquitous presence within these systems [1–3]. Bacterial based biofouling refers to the natural, albeit sometimes undesirable, process through which a complex microbiological system (termed biofilm) forms upon a surface. Biofilms typically consist of a diverse array of microbial cells and colonies embedded within a highly hydrated, protective polymer matrix of which extracellular carbohydrates and proteins dominate. Any pipe conveying a liquid is potentially susceptible to biofilm development and biofouling to some degree as bacteria, fungi, mosses and invertebrates seek to exploit the desirable growth conditions that the pipe surface provides.

Biofilms have the ability to impair a system's hydraulic efficiency through an increase in boundary shear stresses and surface roughness [4,5], and can have a detrimental impact on water quality [1,2,6]. Such water quality issues caused by biofilm development within DWDS may include impaired taste, odour and colour; in addition to causing potential health problems to consumers, ranging from viral and bacterial gastro-enteric diseases, to infections such as hepatitis A and giardiasis [1,2]. In particular, biofilms can contribute and/or exaggerate the accumulation of iron and manganese. This represents a major problem to the water industry as their presence within the water column contributes significantly to discolouration [2,6]. Biofilm development may also contribute to undesirable corrosion and nitrification issues, depending on the pipe material. Within DWDS, the impact of biofouling on surface roughness is considered to be of secondary importance, especially concerning the aforementioned water quality issues. This is because poor water quality will generally result in more customer complaints. Furthermore, water quality is usually compromised by a very thin biofilm (<30 µm), and therefore, it is the general practice of asset holders to make use of disinfectants and flushing techniques to minimise biofouling within DWDS. However, biofilms are known to have a high resilience to these control measures [1]. Moreover, even a relatively thin biofilm (<160 µm) can potentially cause a considerable increase in frictional resistance [5], particularly in long pipe runs. Early observations [7,8] within water mains highlighted the potential impact that biofouling can have on the surface roughness of DWDS, despite the reported biofilm thicknesses (1.0–9.4 mm) being unrepresentative of biofilms typically found within modern, well

maintained DWDS (which seldom exceed 1 mm). Furthermore, the resultant decreases in flow capacity within DWDS because of biofouling will also increase the planktonic (free-floating) bacteria concentrations; through an increase in the pipelines hydraulic retention time (HRT) [9]. Consequently, the water quality is impaired and the likelihood of further fouling and/or other fouling issues (e.g. public health problems) is increased.

The development, behaviour and population characteristics of a biofilm can be influenced by their intrinsic biological properties, along with a number of environmental factors including the velocity field of the fluid in contact with the microbial layer [1]. Hydrodynamic conditions will determine the rate of transport of cells, oxygen and nutrients to the surface, as well as the magnitude of the shear forces acting on a developing biofilm. This is due to its influence on mass transfer, drag and diffusion. In a related study by Lehtola *et al.* [10], the effects of flow velocity on the formation of biofilms indicated that the formation of biofilms increased with the flow velocity and that the mass transfer of nutrients played a major role in the growth of the biofilms.

The mass transfer, drag and diffusion potentials of a system are predominantly controlled by the level of turbulence in the flow, which is conventionally estimated by the dimensionless parameter Reynolds number, Re . Biofilm thickness can be limited by stable and high flow regimes owing to higher shear stresses [11]. However, such conditions typically induce biofilms that are more cohesive and less prone to detachment than those cultivated at low and stable flow regimes. Flow hydrodynamics may also influence the amount and type of extracellular polymeric substances (EPS) found within a biofilm [12]. The hydraulic conditions in DWDS vary daily and seasonally from stagnation to high flow as demand varies and these variances are reflected in the resultant biofilm.

This study addresses these issues with the main aim of examining the effect of the combined interaction of the physical and hydraulic conditions of DWDS on biofilm development in a range of different pipe materials. This will enable the understanding and identification of pipe materials that are prone or resistant to biofilm development. Moreover, such information will allow the manipulation of hydrodynamic conditions to be used as a control parameter to improve strategies for biofilm management.

2. Materials and methods

2.1 . Experimental facility

In this study, a flow cell arrangement was used (Figure 1) to simulate the conditions of a pipeline. The design of

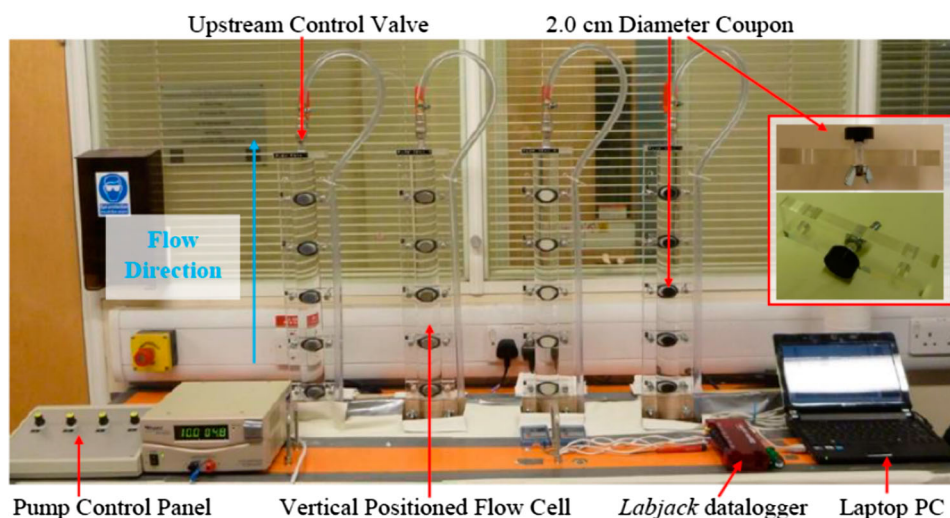


Figure 1. Flow cell configuration used in this study.

which was based on concepts outlined by Teodósio *et al.* [13] and Pereira *et al.* [14]. The ability of a flow cell styled reactor to mimic the hydrodynamic conditions within a pipeline have been well documented through numerical and physical investigations [13]. The configuration and key characteristics of the flow cell used in this study are shown in Figure 1 and Table 1, respectively. The flow cell system consisted of a 10 L maximum capacity recirculating tank, one vertically positioned flow cell, a clear PVC recirculation tube, an inline turbine flow metre (RS 511-4772) and a 0.33 kW centrifugal water pump (Clarke CEB102). Flow cells were positioned vertically to minimise trapped air within the system.

Along the planar surface of the flow cell, there were five equally spaced apertures to fit five removable circular adhesion coupons, each measuring 20 mm in diameter. The first aperture was positioned 51.5 cm from the flow cell inlet. The four remaining apertures were positioned every 10 cm from the first. The purpose of this separation was to minimise potential disruptions in boundary shear caused by the respective downstream coupons. The last aperture was located 0.15 m from the flow cell outlet. A simulation of the flow cell

arrangement used in this study by numerical methods using computational fluid dynamics (CFD) indicated that 0.5 m was a sufficient length for fully developed flow to be obtained within the system (for the full range of operating conditions).

Adhesion coupons were fabricated from representative and commonly used pipe materials, including polyvinyl chloride (PVC), polypropylene (PP), structured wall high-density polyethylene (Str-HDPE) and solid wall high-density polyethylene (S-HDPE). The coupons were held in place by a uniquely designed holding bracket that allowed for independent adjustments to the position of the coupons. This ensured that each coupon was perfectly flush with the internal surface of the flow cell during testing. Any protrusions would have had an adverse effect on the boundary shear conditions and influence the resultant biofilm development. The design of the flow cell and holding brackets also allowed for individual sampling of the discrete coupons at any given time interval. Where possible, the discrete coupons were cut from actual pipes and therefore, the surface finishes inherent to the respective pipe material's fabrication process were accurately assessed, thereby reducing any potential bias. The coupons were imaged using an Environmental Scanning Electron Microscope (ESEM) before incubation in the bulk water in order to evaluate their respective surface finishes.

The flow rate within each of the discrete systems was independently controlled using two ball valves. The valves were located at the inlet and outlet sides of the respective flow cells. The water temperature within the flow cell systems was regulated using an external cooling unit (DC-750 Refrigerated Cooler, D-D The Aquarium Solution Ltd.), and it was measured using a universal temperature probe (EI-1034 Temperature

Table 1. Key characteristics of the flow cells.

Parameter	Value
Material	Acrylic
k_s	0.009 mm
Hydraulic Diameter	2.44 cm
Flow Area	6.28 cm ²
Wetted Perimeter	10.28 cm
Hydraulic Radius	0.61 cm
Length	100.00 cm
Internal Volume	628.32 cm ³
Volume/Area	100 cm
Biofilm Sampling Points	5
Biofilm Sampling Area	3.14 cm ²

Probe, LabJack Corporation). The external cooling unit was capable of cooling volumes of between 200 and 600 L to within $\pm 1^\circ\text{C}$, over the temperature, T range of $4^\circ\text{C} < T < 28^\circ\text{C}$. All data was recorded using a multifunction 24-bit data logger (U6-Pro; LabJack Corporation), and this was coupled to a purpose built interface developed using the DAQ factory (AzeoTech) data acquisition software. Appropriate sampling times were derived for the respective measurements using a cumulative average approach.

2.2. Operating conditions

Two separate (steady state) flow regimes were evaluated within two individual flow cells, namely a high and low flow assay. The two regimes were $Re = 3.41 \times 10^3$ (low flow assay) and $Re = 5.35 \times 10^3$ (high flow assay). The average freestream velocities, \bar{U} , within the two flow cells during low and high flow assays were 0.16 and 0.24 m/s, respectively. The shear forces, τ_w acting on the biofilms within the low flow and high flow assays were 0.13 and 0.24 N/m^2 , respectively. These values were based on the initial conditions (without biofouling), and the principle that the primary shear force acting on the biofilm was the shear force generated by the flow [15]. Husband *et al.* [2] reported that the average values of \bar{U} , Re and τ_w within DWDS in the UK are 0.06 m/s, 4.2×10^3 and 0.28 N/m^2 , respectively. Using this information, Husband *et al.* [2] and later, Douterelo *et al.* [1] cultivated biofilms within a 203 m long pilot scale pipeline across the range of $0.2 \text{ N/m}^2 < \tau_w < 9.10 \text{ N/m}^2$. In a similar investigation, Manuel *et al.* [16] incubated drinking water biofilms within a flow cell reactor at $\bar{U} = 0.21 \text{ m/s}$ and $Re = 5.0 \times 10^3$. The shear forces induced by the respective flow regimes employed within the current study are therefore, comparable to similar studies and representative of actual systems.

In order to provide representative water chemistry, the flow cells were connected to the local (Cardiff, UK) drinking water distribution system by a trickle feed (and drain). The trickle was set to give an overall system HRT of 12 h. The internal HRT within the high and low assays were 79 and 109 s, respectively and as a result, both systems were considered to be well mixed. The pH of the water within the flow cells during incubation was close to neutral (7.60 ± 0.25), whilst the temperature ranged from 14.8–15.6°C during incubation.

The maximum recorded values of total organic carbon and dissolved organic carbon were 4.10 and 3.30 mg/L, respectively. The free chlorine concentration in the system was close to the lower range within a typical UK DWDS [1,2]. However, this was expected, as chlorine

decreases with time due to its reactive nature, and would be naturally lower towards the end of the system.

The flow cell systems were disinfected using a concentrated chlorine solution ($\text{Cl} = 2 \text{ mg/L}$) based on the published protocol [1]. Essentially, the systems were flushed with chlorine at the maximum flow rate (2100 L/h) for 48 h. Thereafter, the bulk water within the systems was allowed to stand for a further 24 h before further flushing with fresh water. The water within the facility was replaced until the levels of free chlorine were within local drinking water limits. Preliminary testing identified that the average concentration of free chlorine within the local DWDS was approximately 0.04 mg/L. The coupons were independently sterilised prior to testing to remove residual bacteria and impurities. This was achieved by immersing the coupons in 80% (v/v) ethanol for 12 h, and left to dry in a clean fume cupboard for a further 24 h.

2.3. Biofilm sampling and analysis

Samples of biofilm were collected from the flow cells after 100 d. At the point of sampling, the flow within each of the respective flow cells was stopped and the bulk water sealed within them by closing the inlet and outlet valves. The discrete flow cells were detached from the recirculating system and placed planar side up on a surface sterilised bench (washed with 80% (v/v) ethanol). The adhesion coupons were then removed and the biofilm sampled aseptically by removing 75% (approximate area: 2.4 cm^2) of the biofilm from each of the coupons using a sterile cotton swab (Fisher Scientific UK Ltd.). The cotton bud was cut from the swab and aseptically transferred to a sterile 1.5 ml APEX® NoStick™ microcentrifuge tube (Alpha Laboratories Ltd.). All biofilm samples were stored at -80°C until required for DNA extraction. The coupons and remaining biofilm (approximate area: 0.8 cm^2 or 25%) were then sputter-coated with gold and examined under a Veeco FEI (Philips) XL30 Environmental Scanning Microscope (ESEM).

2.4. Environmental scanning electron microscopy (ESEM)

The physical surface roughness of the coupons with and without fouling was determined using ESEM and the image analysis software, MountainsMap version 7 (Digital Surf). The image software estimated the surface topography using a 'single four image scan' approach as per the manufacturer's specification. Eight randomly selected $0.5 \times 0.5 \text{ mm}^2$ sampling areas were assessed for each coupon.

The surface roughness of a material can be defined by a number of statistical parameters, including: mean roughness height, k_{av} ; maximum peak-to-trough height, $k_t (= r_{max} - r_{min}$ where r is the distance from the mean roughness height); root-mean-square roughness height, $k_{rms} (= \sqrt{1/\sum_{i=1}^N r_i^2}$; where N is the sample number); skewness of the roughness distribution, $s_{kl} (= \left(1/N \sum_{i=1}^N r_i^3 \left[(1/N) \sum_{i=1}^N r_i^2 \right]^{3/2} \right)$ and kurtosis of the roughness distribution, $k_u (= \left(1/N \sum_{i=1}^N r_i^4 \left[(1/N) \sum_{i=1}^N r_i^2 \right]^2 \right)$. The aforementioned parameters for defining physical roughness have been related with varying success to equivalent roughness scales, namely k_s [17]. It has been documented that an engineered surface can be related to k_s by using k_{rms} and s_{kl} [18] or by using k_{rms} on its own [19]. However, the relationship reported by Flack and Schultz [18] is for surfaces with relatively high k_s values ($k_s > 500 \mu\text{m}$). For an engineered material with a small k_s value ($k_s < 10 \mu\text{m}$), the following relationships are typically applied [19,20]:

$$k_s \approx 5k_{rms}; \quad (1)$$

Or

$$k_s \approx 3k_{rms} \quad (2)$$

However, which relationship is used is dependent on the surface finish of the material in question. For instance, Equation 1 [20] is to be used for machine finished surfaces with an approximate Gaussian roughness distribution, whereas, Equation 2 [19] was suggested for materials such as aluminium or steel which have been honed and polished. Based on Equations 1 and 2, and a k_s value of 0.012 mm, the k_{rms} of the test pipe was estimated to be between 2.4 and 4 μm .

2.5. DNA extraction and purification

Total community genomic DNA was extracted from each of the biofilm samples directly from the cotton swabs using a Nexttec DNA Isolation Kit for Bacteria (Nexttec Biotechnologie GmbH). The procedure was per the manufacturer's instructions with the exceptions that after adding Buffer, Lysozyme and RNase A; the sample was mechanically shaken using a multi-wrist shaker (Lab Line) at maximum speed for 5 min, and the final extracted DNA was eluted in 200 μl of molecular grade water (Severn Biotech Ltd.). The DNA extracts were then stored at -80°C until required for Polymerase Chain Reaction (PCR) amplification. DNA extractions were also carried out on unused sterile cotton swabs as negative controls.

2.6. PCR conditions

To minimise potential contamination, PCR was carried out under aseptic conditions using autoclaved and/or UV-treated plasticware and equipment. Bacterial 16S rRNA genes were amplified using primers 357FGC and 518R [21]. All PCR were performed within a DNA Engine Dyad Thermal Cycler (MJ Research) using conditions as described [21]. Sterile nuclease-free molecular-grade water and Acetobacterium species Ac1 [22] DNA were used as negative and positive controls, respectively in all sets of PCRs. Reaction mixtures were held at 95°C for 5 min followed by 10 cycles of 94°C for 30 s, 55°C for 30 s and 72°C for 60 s; plus 20 cycles of 94°C for 30 s, 52°C for 30 s and 72°C for 60 s, with an extension step of 5 min at 72°C .

2.7. DGGE analysis and sequencing excised DGGE bands

To determine the bacterial diversity within the biofilm samples, Denaturing Gradient Gel Electrophoresis (DGGE) was carried out on the PCR products [23,24]. The PCR products were separated using a DCode Universal Mutation Detection System (Bio-Rad Laboratories), and 1.0 mm thick ($16.0 \times 16.0 \text{ cm}^2$ glass plate) 8.0% (w/v) polyacrylamide gels (40% w/v acrylamide solution, acrylamide: N,N'-methylenebisacrylamide; 37.5:1; Severn Biotech Ltd.), with denaturant gradient between 30% and 60% [21]. The polyacrylamide gels were prepared with a 1x Tris-Acetate EDTA (TAE) buffer (pH 8) using a 50 ml volume Gradient Mixer (Fisher Scientific UK Ltd.). Electrophoresis was performed at 60°C and 200 V for 5 h (with an initial 10 mins at 80 V). The polyacrylamide gels were stained with SYBRgold nucleic acid gel stain (Invitrogen) for 30 mins and viewed under UV using a Gene Genius Bio Imaging System (Syngene). Distinguishable DGGE bands were excised, washed and re-amplified by PCR [25] for Sanger sequencing by Eurofins Genomics.

2.8. Total DNA quantification and estimated cell numbers

The total DNA concentration was measured within the biofilm and bulk water samples volume using a fluorescent dye assay kit (Quant-iT PicoGreen dsDNA Assay Kit; Invitrogen) and a multimode microplate reader (Infinite200 Pro; Tecan Group Ltd.). Samples and standard curves were prepared on a 96 microplate (Opti-Plate-96F, black; PerkinElmer Inc.) as per the manufacturer's specification and the microplate was

read using the pre-defined PicoGreen programme (Magellon 7.1). Samples were excited at 485 nm and fluorescence intensity was measured at 535 nm. All standard curves used within the study had R^2 of at least 0.99. A strong linear relationship has been reported within the literature between DNA concentration and total direct cell counts [26]. The recommendations outlined [26] were used within the current study to estimate the total cell number within biofilm samples.

3. Results and discussion

3.1. Surface roughness

3.1.1. Pre-incubation

The results of the physical roughness evaluation for the four different materials are presented in Table 2. The surface roughness parameters represent the total mean values from eight replicate profiles. Figure 2 presents typical micro-topography (area: $0.5 \times 0.5 \text{ mm}^2$) of each of the coupons pre-incubation. It is evident from Figure 2 that the surface micro-geometry of the four materials differs when viewed under ESEM. For example, the surface of the PVC and Str-HDPE coupons appeared to be covered with numerous scratches, grooves and deformation marks (Figure 2c & 2d). Whereas, the surface of the PP coupon appeared free from deformations and was extremely smooth (Figure 2a).

The roughness parameters listed in Table 2 show that the Str-HDPE coupon had the highest roughness of the assessed coupons, with average k_{av} of $3.70 \mu\text{m}$. The PP coupon was statistically the smoothest of the five coupons, with an average k_{av} of $0.59 \mu\text{m}$. Ranking the respective materials based on their physical roughness yields $\text{PP} < \text{S-HDPE} < \text{PVC} < \text{Str-HDPE}$. Presumably, the increased roughness of the Str-HDPE coupon would aid microbial attachment and biofilm formation, whereas, the relatively smooth nature of the PP coupon would limit biofilm development [27]. The relationship between the value of k_{rms} and the actual value of k_s for the S-HDPE pipe was found to be approximately equal to the relationship proposed [19] (Equation 2).

Table 2. Pre-incubation physical roughness parameters of PP, S-HDPE, PVC and Str-HDPE coupons.

Material	k_{av} (μm)	k_t (μm)	k_{rms} (μm)	s_{kl}	k_s (μm) (Predicted)*
PP	0.59	24.10	0.85	2.24	2.55
S-HDPE	1.47	23.50	2.22	2.78	6.66
PVC	2.28	28.80	3.08	1.60	9.24
Str-HDPE	3.70	29.40	4.97	1.49	14.91

* $k_s \approx 3k_{rms}$ [19].

3.1.2. Post incubation

After 100 d incubation, ESEM imaging clearly identified the major components of the biofilms formed on pipe materials when exposed to drinking water. In particular, biofilms consisted predominantly of sparse populations of rod-shaped colonising bacteria embedded within the EPS-like material (Figure 3). In addition, small numbers of filamentous bacteria were also evident as shown in Figure 3e. Similar to observations made by Percival et al. [28] for biofilms incubated with drinking water when viewed under Scanning Electron Microscopy (SEM). Furthermore, the 'fibrillar strand' structures of EPS observed [28] were also observed in this study, particularly on the PVC coupons as shown in Figure 3d. However, the previous study [28] also observed small numbers of fungi, yeast cells and diatoms; none of which were evident in the images captured within the current study.

Furthermore, the ESEM images also showed that various amounts of microbial material with very different biofilm morphologies were present depending on the pipe material and flow hydrodynamic conditioning (see Figures 4 and 5). Typically, the amount of microbial biomass on the coupons was greater within the low flow assay than within the high flow assay (Figure 4). Additionally, it can be seen that biofilms incubated within the high flow assay were seemingly more isolated than those within the low flow assay. It is expected that if the overall shear conditions remain below the critical level, biofilms conditioned at high shear will show more rapid and extensive development than those conditioned at low shear, due to mass transfer and diffusion principles [16,28]. Furthermore, the high mass transfer potential associated with high shear conditioning will generally induce a less isolated and more uniformly distributed biofilm [28]. Nevertheless, the inherently low nutrient conditions within drinking water will likely negate the influence of mass transfer and diffusion on biofilm development, due to the overall lack of biological material present [29]. The increased mass transfer and diffusion associated with high shear conditioning will also encourage the influx of disinfectants (if used). However, it should be noted that the observations made by Percival et al. [28] about the fostered biofilm uniformity at high shear conditioning were for a drinking water system. Nevertheless, it is evident from the current study that biofilm development within a drinking water environment is inhibited at high shear, which suggests that the overall shear forces imposed by the flow were above the critical levels.

In terms of the discrete materials, the PVC and Str-HDPE coupons showed the largest amounts of microbial biomass, irrespective of the flow conditions. These

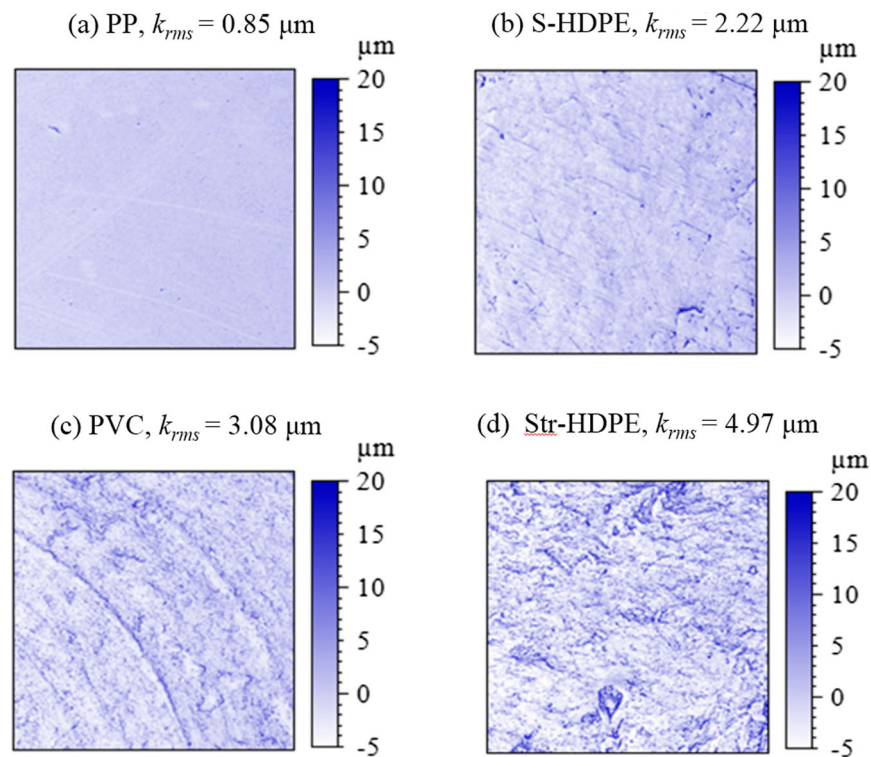


Figure 2. Pre-incubation micro-topography maps viewed under ESEM of (a) PP, (b) S-HDPE, (c) PVC and (d) Str-HDPE coupons (size: $0.5 \times 0.5 \text{ mm}^2$ and magnification: $\times 200$). k_{rms} = root-mean-square roughness height (mm).

materials also showed the greatest initial roughness of the four coupons (Table 2). The morphology of the respective biofilms incubated on the PVC and Str-HDPE coupons; however, differed considerably between the two materials. The biofilms incubated on the PP and S-HDPE coupons showed similar morphologies and were comprised of similar amounts of microbial material. Based on similar observations on biofilms incubated with drinking water on different pipe materials, Yu et al. [30] suggested that surface roughness can have a considerable impact on biofilm formation, and that materials which are initially rough, will foster greater biofilm development.

The coupon images captured by ESEM after incubation with drinking water were analysed using the MountainsMap software. The results of the physical roughness evaluation of the coupons post incubation are presented in Figures 4 and 5. A change in roughness was observed in all cases post incubation. The change in physical roughness post incubation is a function of the biofilms structure, and in particular its thickness. Typically, an increase in roughness is fostered by an increase in thickness. However, this is not always the case, and in some instances, biofilms have smoothen an initially rough surface by filling its cavities and grooves [17]. Such growth practices are common in low-level fouling systems. On this basis, the surface

of a DWDS could potentially be smoothened by biofilm development; and consequently, it could improve the system's hydraulic performance. The smoothening of a surface typically involves reduction in the maximum valley or pit height [17]. This was however not the case for any of the assessed materials incubated with drinking water in the current study. As a result, an increase in physical roughness post incubation was reported for all the materials. For instance, k_{rms} for the PP coupon increased from $0.85\text{--}5.86 \mu\text{m}$ following incubation. Similarly, the k_{rms} for the Str-HDPE coupon increased from $4.97\text{--}7.39 \mu\text{m}$ following incubation. Nonetheless, the observed increases in roughness caused by the biofilm would have had negligible effect on a system's hydraulic performance and equivalent roughness. For instance, the Str-HDPE coupon had the greatest amount of microbial growth. Giving that the k_s induced by a biofilm is 1.5 times greater than its k_t [17]; the k_s imposed by the surface with fouling would have been between $0.048\text{--}0.050 \text{ mm}$ depending the conditioning shear (i.e. $k_t = 32.3\text{--}33.6 \mu\text{m}$).

3.2. Biofilm DNA concentration

Following incubation with drinking water for 100 d, the microbial DNA concentrations extracted from the

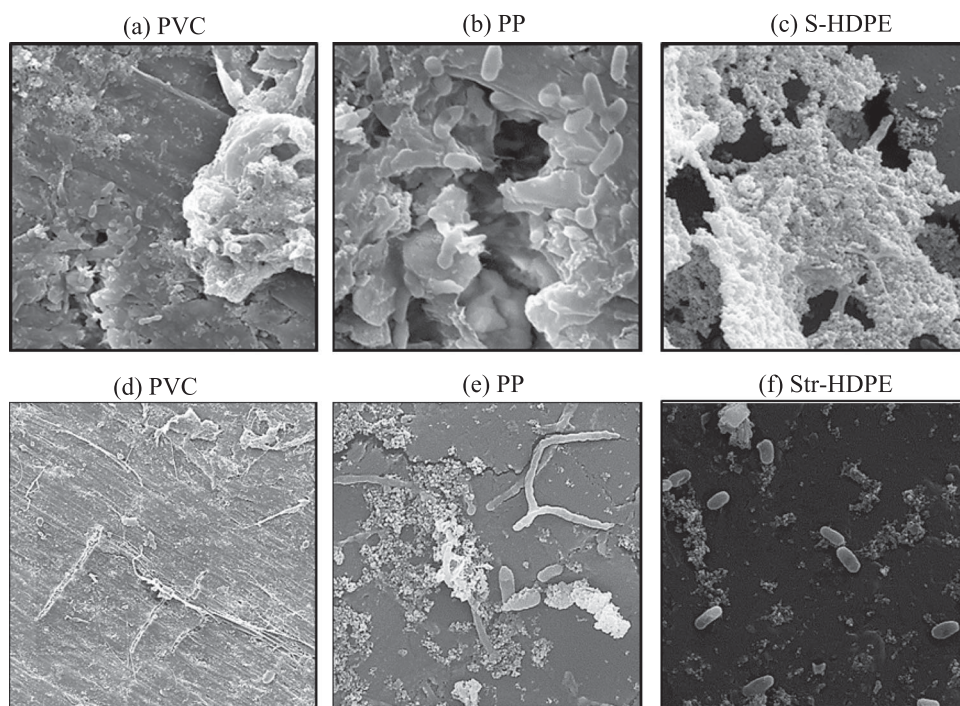


Figure 3. ESEM micrographs of different pipe material coupons post incubation. (a) PVC at $\times 5000$ magnification, (b) PP at $\times 20,000$ magnification, (c) S-HDPE at $\times 20,000$ magnification, (d) PVC at $\times 650$ magnification, (e) PP at $\times 20,000$ magnification and (f) Str-HDPE at $\times 20,000$ magnification.

discrete coupons ranged from 5.28–45.60 ng/cm² (Figure 6). The estimated cell concentrations on each of the coupons ranged from 4.0×10^5 – 3.7×10^6 cells/cm². This concentration range is similar to that reported by Niquette et al. [31], who found that the total cell concentration on plastic-based materials (including PE and PVC) when incubated with drinking water with low levels of residual chlorine (< 0.05 mg/L) ranged from 7.0×10^4 – 5.0×10^5 cells/cm². In contrast, Manuel et al. [16] found that the cell concentration on coupons fabricated from HDPE and PVC when incubated with drinking water under shear conditions in excess of those reported within the current study were an order of magnitude higher (i.e. $\tau_w = 0.80$ – 1.91 N/m²) and ranged from 2.6×10^7 – 8.7×10^7 cells/cm².

The DNA and total estimated cell concentrations were consistently lower within the high flow assay compared to the low flow assay. The magnitude of the difference between the high and low flow assay DNA concentrations was seemingly dependant on the pipe material. For example, the greatest difference in DNA and therefore cell concentrations between flow regimens occurred on the PP coupon, which was the smoothest material assessed. In this particular case, the percentage difference between the high and low flow assay was 108%. The lowest difference in DNA and cell concentrations was found to be 14%, and

this was determined for the material with the highest initial roughness (Str-HDPE). These observations further support the assertion that a smooth material will typically induce higher near-wall velocities and provide less protection and attachment areas, than a rough material. Consequently, the smooth surface characteristics of the PP coupon would have magnified the impact of the increased shear conditions inherent within the high flow assay and therefore, contribute to the greater difference between the low and high flow assay biofilms characteristics.

The S-HDPE and PVC coupons showed intermediate levels of the respective parameters. The DNA concentrations on the S-HDPE coupons were 2.4–3.8 times lower than the equivalent concentrations on the Str-HDPE. The only difference between the respective HDPE materials was surface roughness (Table 2). This suggests that the initial surface roughness of a material can have a significant influence on microbial adhesion and subsequent colonisation. This is because the cavities and grooves, which form a material's surface roughness, will typically influence the transport and attachment of microbial cells by increasing the mass transfer potential, providing shelter from the adverse shear conditions and increasing the attachment area [28,32]. Consequently, numerous studies have found that materials initially high in roughness support

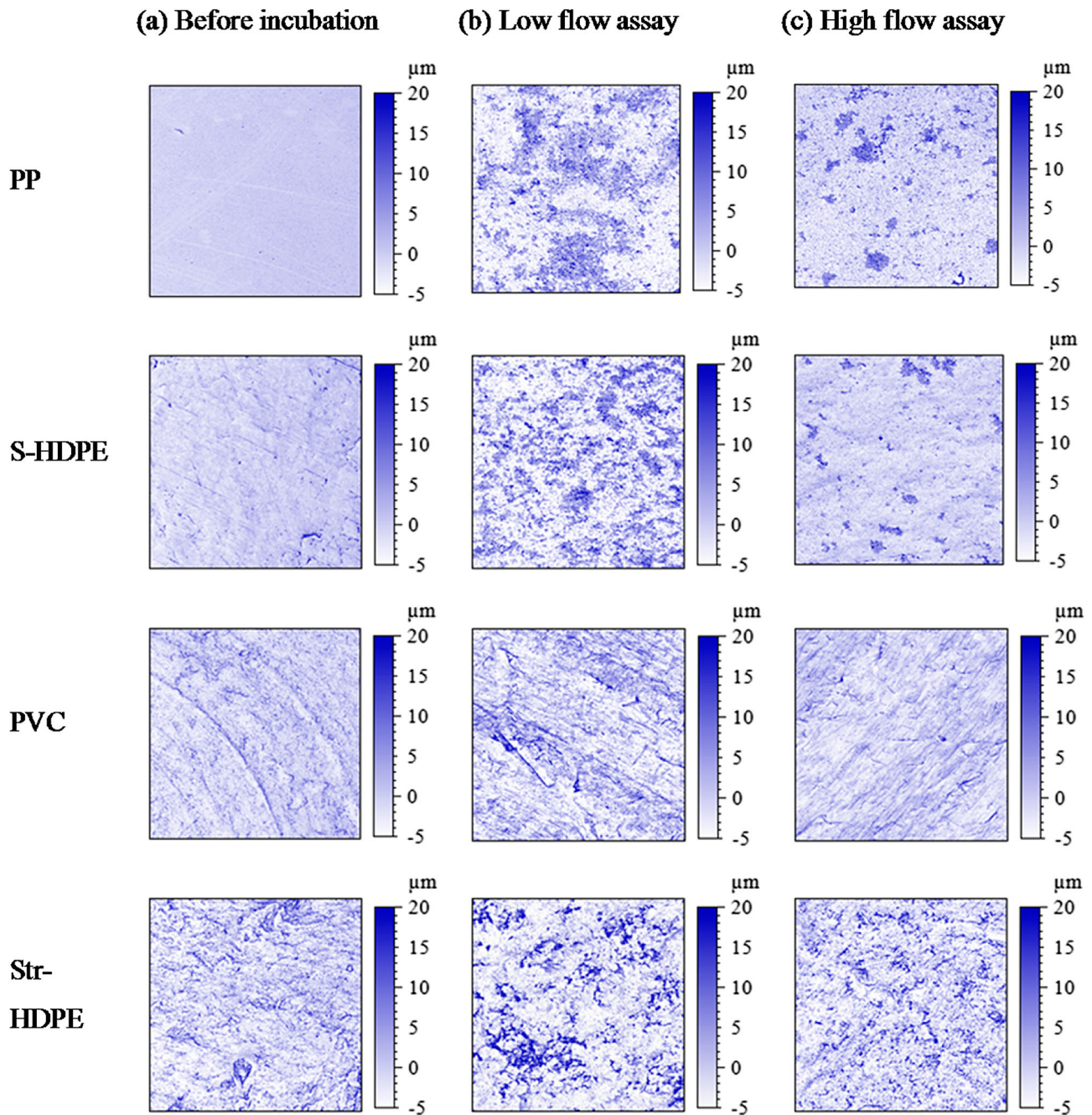


Figure 4. ESEM micrographs of the PP, S-HDPE, PVC and Str-HDPE (a) before incubation and after incubation within the (b) low flow assay (c) high flow assay ($\times 200$ magnification).

significant amounts of biofilm development over the short and long term [30].

3.3. Biofilm bacterial community structure

The dominant bacterial communities within the biofilms incubated on the different pipe material coupons were identified by 16S rRNA gene PCR-DGGE (Figure 7). It should be noted that careful consideration of negative controls during the DNA extraction and PCR-DGGE revealed that sequences related to *Bacillus* species

were found as a contaminant within the cotton buds used for sampling the biofilm and therefore, these sequences were not included in the discussions herein.

Results indicate that the dominant bacterial phyla within biofilms incubated with drinking water were Alphaproteobacteria, Betaproteobacteria and Gammaproteobacteria. Members of the Proteobacteria have been reported previously as the dominant constituents within DWDS biofilms [12,30,33]. The bacterial phylum Cyanobacteria was also found to be present, although only on the S-HDPE coupon at high flow conditions. At

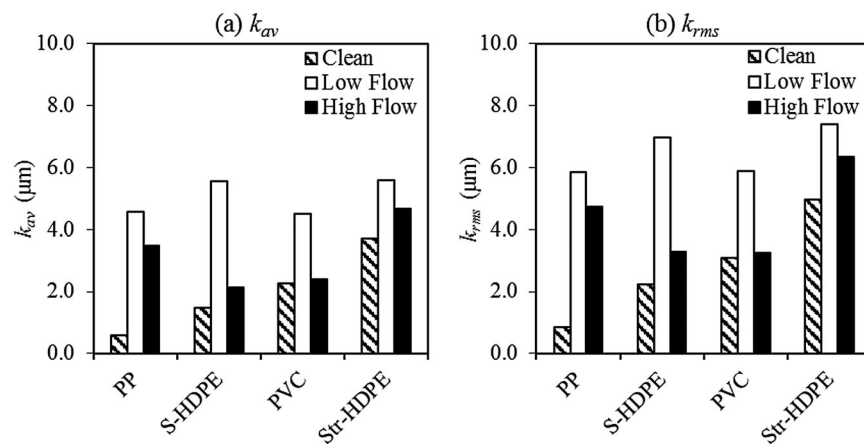


Figure 5. Pre and Post incubation physical roughness parameters for PP, S-HDPE, PVC and Str-HDPE coupons. (a) k_{av} , mean roughness height and (b) k_{rms} , root-mean-square roughness height.

the genus level, bacteria belonging to *Pseudomonas*, *Sphingomonas* and *Aquabacterium* were found to be abundant within most biofilms (Figure 7b). The results further revealed that the characteristics of the biofilm communities varied depending on the material and hydrodynamic conditions used (Figure 7). For example, Alphaproteobacteria was the predominant bacterial group within the biofilms incubated in the low flow assay, and represented 48% of the total number of phylotypes. Gammaproteobacteria (33%) and to a lesser extent Betaproteobacteria (19%) were also found within the low flow assay. In the high flow assay, Betaproteobacteria (45%) and Gammaproteobacteria (33%) were the dominant bacterial groups with Alphaproteobacteria only representing 11% of the population.

Previously, members of the Betaproteobacteria have been documented to have a greater ability than other bacterial groups to attach to a surface and form biofilms within DWDS [34]. Consequently,

Betaproteobacteria and typically *Aquabacterium* species dominate biofilm processes in DWDS. This could explain their abundance within the biofilms incubated within the current study. The presence of Alphaproteobacteria within the respective biofilms could be explained by their known resilience to the commonly used disinfectant, chlorine. In particular, Alphaproteobacteria have a stronger resistance to known disinfectants than other bacterial groups found within DWDS and as a result, they are typically found in abundance in both planktonic and biofilm growth phases of such systems, [1]. *Sphingomonas* and *Pseudomonas* species were the predominant known pathogens found in the biofilms, and in particular, were found to be abundant within the biofilms incubated within the low flow assay. The abundance of such species confirms the potential of biofilms to act as a reservoir for human opportunistic pathogens, which if mobilised into the water column could result in health and disease issues

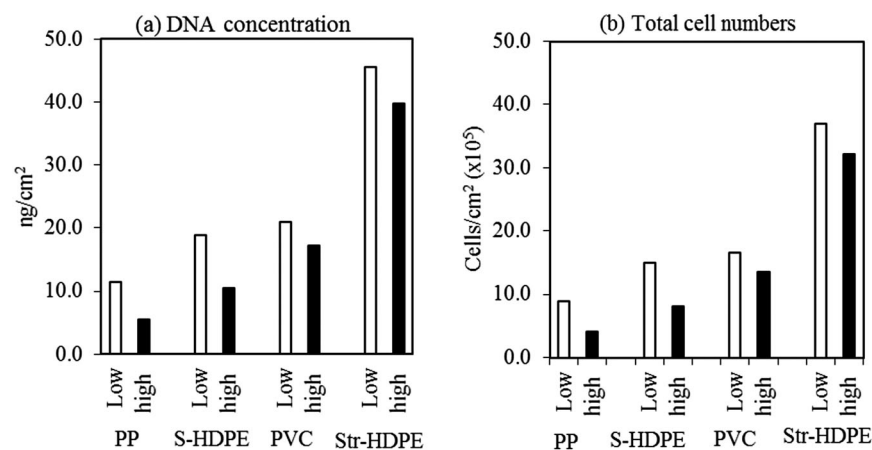


Figure 6. Post incubation (a) DNA concentration and (b) total estimated cell numbers for the PP, S-HDPE, PVC and Str-HDPE coupons (both high and low flow assay systems).

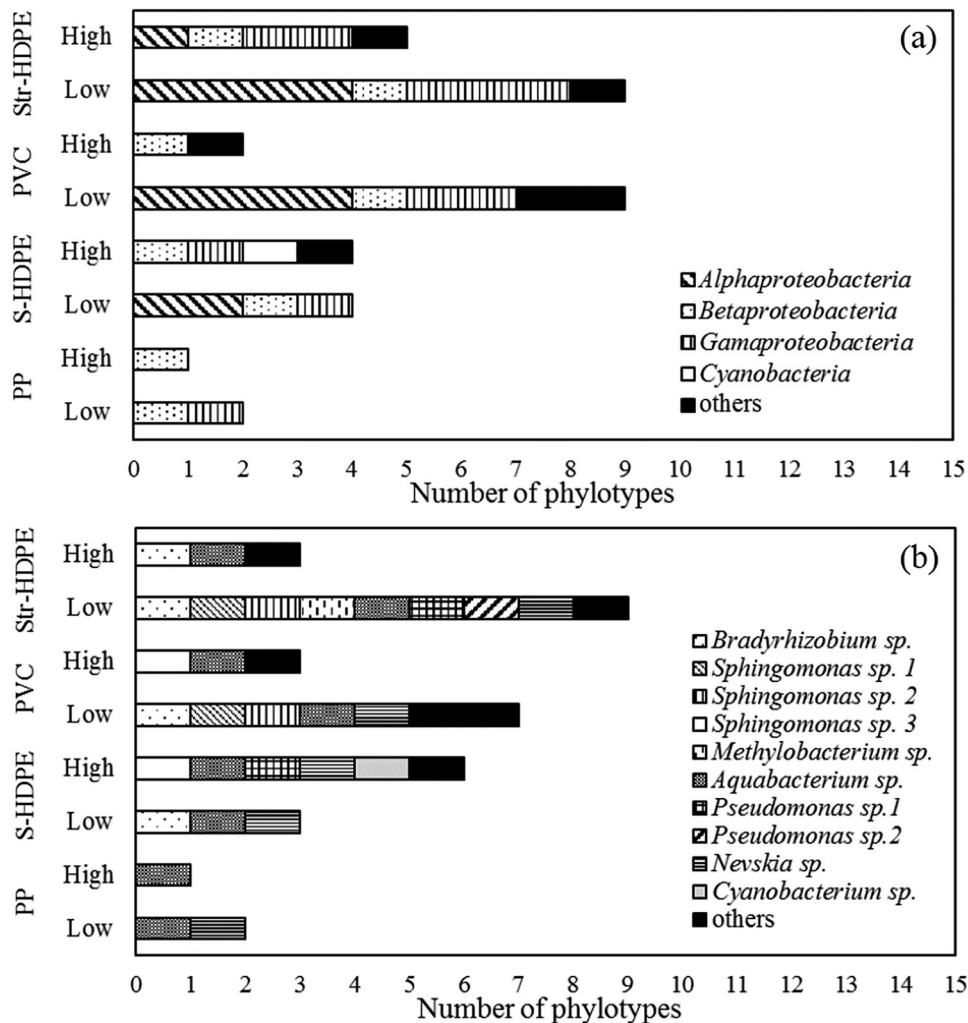


Figure 7. Post incubation bacterial community composition of the PP, S-HDPE, PVC and Str-HDPE coupons (both high and low flow assay systems) determined by 16S rRNA gene PCR-DGGE. (a) Phylum/class level (b) Genus level. Others represent all unidentified DGGE bands.

for consumers, particularly for the young, elderly and the infirm [1]. *Sphingomonas* are typically observed in abundance within DWDS and are known to have a high ability to form bacterial aggregates and biofilms in order to protect against disinfectants, as well as survive under low nutrient concentrations and metabolise a wide variety of toxic compounds [1,30]. The dominance of *Pseudomonas* within DWDS is generally explained by its ability to produce high amounts of cohesive EPS [12,35,36] and as a result they are typically the most abundant bacterial species within DWDS irrespective of the pipe's ecology [1,28]. However, in contrast to such previous findings [1,30], *Pseudomonas* were rarely found within the biofilms incubated within the high flow assay. Interestingly, in the high flow assay, sequences belonging to *Pseudomonas* were only evident within biofilms incubated on the Str-HDPE pipe material (Figure 7b). This suggests that these species have a limited ability to propagate within biofilms

under high shear conditions ($\tau_w > 0.24 \text{ N/m}^2$) without sufficient protection (i.e. roughness). This is supported by the study of Simoes et al. [37] who demonstrate that, although *Pseudomonas* species produce large amounts of EPS, the EPS they produce has a poor mechanical stability under high shear stress. The fact that these potential pathogens were only consistently evident on the Str-HDPE coupon within the high flow assay, suggests that a property inherent within HDPE fostered their development. Douterelo et al. [1] found that *Pseudomonas* species were abundant within biofilms incubated at shear forces in excess of 0.24 N/m^2 . However, the pilot scale pipeline in which the biofilms were incubated was fabricated from HDPE.

In addition to the protection of biofilms offered by Str-HDPE, there is also conflicting evidence within the literature on whether or not PE-based pipes release biodegradable organic compounds and phosphorus [12]. This could provide nutrients to support biofilm

development within DWDS which members of the genera *Pseudomonas* could particularly exploit given their highly metabolically versatile nature [38]. It is also possible that *Pseudomonas* species could be causing the release of nutrients due to their high enzyme activity, as highlighted by their use in the biodegradation of plastics [38]. There is evidence to suggest PE-based materials do release such compounds [30]; and there is equally compelling evidence to suggest that they do not [16]. The low overall system HRT meant it was not possible to determine if any leaching or biodegradation did occur within the current investigation. Therefore, it is suggested that further work is undertaken to investigate the potential of HDPE to harbour greater concentrations of pathogens and opportunistic microbes compared to other plastic-based materials.

4. Conclusions

This study has expanded on the current knowledge relating to the impact of surface roughness and flow hydrodynamic conditions on biofilm development within drinking water distribution systems. Surface roughness and flow hydrodynamics are linked by basic boundary layer principles and as a result, the impacts of these factors on biofilm development are naturally related to each other. In this study, the results of the DNA and estimated cell counts indicate that the surface properties, namely roughness of different plastic materials can have a considerable impact on microbial attachment and subsequent biofilm colonisation. This is in contrast to previous investigations, which found that plastic-based materials as a whole support similar amounts of fixed biomass.

The impact of surface roughness on biofilm development was seemingly greater than the impact of flow hydrodynamics, at least for the range of shear stresses of between 0.13–0.24 N/m² and although, this range is relatively small, it is representative of typical DWDS. Furthermore, the concentrations of bacteria were lower in the high flow assay on the smoother coupons than in the low flow assay on the rougher coupons. These observations support the argument that material properties can have a considerable influence on biofilm development within DWDS. However, the inherent relationship between surface roughness and flow hydrodynamics should not be ignored; typically, it was found that the amount of microbial biomass on the coupons was greater and less isolated within the low flow assay than within the high flow assay. Moreover, it is also widely acknowledged that any potential material and flow hydrodynamic impacts are less when high levels of disinfectants are used. Therefore, conclusions drawn are limited to the aforementioned shear conditions and areas of low

chlorine concentration (i.e. < 0.04 mg/L). Such areas are typical at the end of long pipelines or branches.

It is worthy to note that the biofilms incubated for 100 d with drinking water within the current study were extremely thin. If the observed development is representative of biofilms within actual plastic based systems, then it is likely those system's hydraulic performance will be unaffected by biofilm development. However, as it can take several years for a biofilm to reach a state of maturity, it would be ideal for more extensive long-term incubations to be performed using a larger facility capable of measuring small changes in surface roughness.

Acknowledgements

The authors would like to acknowledge the funding support provided by the UK Engineering and Physical Sciences Research Council (EPSRC), Asset International Ltd. and Natural Environment Research Council (NERC). The authors would also like to thank the technical staff at the School of Engineering, Cardiff University, and in particular, Mr Len Czekaj and Mr Paul Leach for their support with the experimental work. All electron microscopy was carried out at the Electron Microbeam Facility, School of Earth and Ocean Sciences, Cardiff University.

Disclosure Statement

No potential conflict of interest was reported by the authors.

Funding

This work was supported by Engineering and Physical Sciences Research Council studentship; Natural Environment Research Council: [grant number NE/J011177/1].

ORCID

Matthew W. Cowle  <http://orcid.org/0000-0002-8141-2685>
Gordon Webster  <http://orcid.org/0000-0002-9530-7835>
Andrew J. Weightman  <http://orcid.org/0000-0002-6671-2209>

Underlying Research Material

Information on the data underpinning the results presented here, including how to access them, can be found in the Cardiff University data catalogue at <http://doi.org/10.17035/d.2019.0075602177>.

References

- [1] Douterelo I, Sharpe RL, Boxall JB. Influence of hydraulic regimes on bacterial community structure and composition in an experimental drinking water distribution system. *Water Res.* 2013;47:503–516.
- [2] Husband PS, Boxall JB, Saul AJ. Laboratory studies investigating the processes leading to discoloration in water distribution networks. *Water Res.* 2008;42:4309–4318.

- [3] Cowle MW, Babatunde AO, Rauen WB, et al. Biofilm development in water distribution and drainage systems: dynamics and implications for hydraulic efficiency. *Environ Technol Rev.* 2014;3:31–47.
- [4] Walker J, Sargison J, Henderson A. Turbulent boundary-layer structure of flows over freshwater biofilms. *Exp Fluids.* 2013;54:1–17.
- [5] Schultz MP, Swain GW. The effect of biofilms on turbulent boundary layers. *J Fluids Eng.* 1999;121:1–22.
- [6] Husband PS, Boxall JB. Understanding and managing discoloration risk in trunk mains. *Water Res.* 2016;107:127–140.
- [7] Seifert L, Kruger W. Unusually high friction factor in a long, water supply line. *VDI Z.* 1950;92:189–191.
- [8] Sharp BB. Examination of the friction in the Morgan-Whyalla pipeline. Adelaide, Australia: Prepared for Engineering & Water Supply Department; 1954.
- [9] Eisnor J, Gagnon G. A framework for the implementation and design of pilot-scale distribution systems. *J Water Supply Res Technol-Aqua.* 2003;52:501–519.
- [10] Lehtola M, Laxander M, Miettinen IT, et al. The effects of changing water flow velocity on the formation of biofilms and water quality in pilot distribution system consisting of copper or polyethylene pipes. *Water Res.* 2006;40:2151–2160.
- [11] Celmer D, Oleszkiewicz J, Cicek N. Impact of shear force on the biofilm structure and performance of a membrane biofilm reactor for tertiary hydrogen-driven denitrification of municipal wastewater. *Water Res.* 2008;42:3057–3065.
- [12] Fish KE, Osborn AM, Boxall J. Characterising and understanding the impact of microbial biofilms and the extracellular polymeric substance (EPS) matrix in drinking water distribution systems. *Environ Sci Water Res Technol.* 2016;2:614–630.
- [13] Teodósio J, Simoes M, Melo L, et al. Flow cell hydrodynamics and their effects on *E. coli* biofilm formation under different nutrient conditions and turbulent flow. *Biofouling.* 2011;27:1–11.
- [14] Pereira MO, Kuehn M, Wuertz S, et al. Effect of flow regime on the architecture of a *Pseudomonas fluorescens* biofilm. *Biotechnol Bioeng.* 2002;78:164–171.
- [15] Stoodley P, Cargo R, Rupp CJ, et al. Biofilm material properties as related to shear-induced deformation and detachment phenomena. *J Ind Microbiol Biotechnol.* 2002;29:361–367.
- [16] Manuel CM, Nunes OC, Melo LF. Dynamics of drinking water biofilm in flow/non-flow conditions. *Water Res.* 2007;41:551–562.
- [17] Andrewartha JM. The effect of freshwater biofilms on turbulent boundary layers and the implications for hydro-power canals [PhD thesis]. University of Tasmania; 2010.
- [18] Flack KA, Schultz MP. Review of hydraulic roughness scales in the fully rough regime. *J Fluids Eng.* 2010;132:041203–041203-10.
- [19] Zagarola MV, Smits AJ. Mean-flow scaling of turbulent pipe flow. *J Fluid Mech.* 1998;373:33–79.
- [20] Hama FR. Boundary-layer characteristics for smooth and rough surfaces. *Trans – Soc Nav Archit Mar Eng.* 1954;62:333–358.
- [21] Webster G, Newberry CJ, Fry JC, et al. Assessment of bacterial community structure in the deep sub-seafloor biosphere by 16S rDNA-based techniques: a cautionary tale. *J Microbiol Methods.* 2003;55:155–164.
- [22] Parkes RJ, Seltek G, Webster G, et al. Culturable prokaryotic diversity of deep, gas hydrate sediments: first use of a continuous high-pressure, anaerobic, enrichment and isolation system for seafloor sediments (DeepISOBUG). *Environ Microbiol.* 2009;11:3140–3153.
- [23] Webster G, Embley TM, Prosser JI. Grassland management regimens reduce small-scale heterogeneity and species diversity of β -proteobacterial ammonia oxidizer populations. *Appl Environ Microbiol.* 2002;68:20–30.
- [24] Webster G, Parkes RJ, Cragg BA, et al. Prokaryotic community composition and biogeochemical processes in deep seafloor sediments from the Peru margin. *FEMS Microbiol Ecol.* 2006;58:65–85.
- [25] O'Sullivan LA, Webster G, Fry JC, et al. Modified linker-PCR primers facilitate complete sequencing of DGGE DNA fragments. *J Microbiol Methods.* 2008;75:579–581.
- [26] McCoy WF, Olson BH. Fluorometric determination of the DNA concentration in municipal drinking water. *Appl Environ Microbiol.* 1985;49:811–817.
- [27] Tsvetanova Z. Study of biofilm formation on different pipe materials in a model of drinking water distribution system and its impact on microbiological water quality. In: Chemicals as intentional and accidental global environmental threats, NATO security through science series. Amsterdam, the Netherlands: Springer; 2006. p. 463–468.
- [28] Percival SL, Knapp JS, Wales DS, et al. The effect of turbulent flow and surface roughness on biofilm formation in drinking water. *J Ind Microbiol Biotechnol.* 1999;22:152–159.
- [29] Stoodley P, Dodds I, Boyle JD, et al. Influence of hydrodynamics and nutrients on biofilm structure. *J Appl Microbiol.* 1998;85:195–285.
- [30] Yu J, Kim D, Lee T. Microbial diversity in biofilms on water distribution pipes of different materials. *Water Sci Technol.* 2010;11:163–171.
- [31] Niquette P, Servais P, Svoir R. Impacts of pipe materials on densities of fixed bacterial biomass in a drinking water distribution system. *Water Res.* 2000;34:1952–1956.
- [32] Costerton JW, Cheng KJ, Geesey GG, et al. Bacterial biofilms in nature and disease. *Annu Rev Microbiol.* 1987;41:435–464.
- [33] Shi Y, Babatunde A, Bockelmann-Evans B, et al. Influence of hydraulic regimes and Cl₂/NH₃-N mass ratio on bacterial structure and composition in experimental flow cell chloraminated drinking water system. *Environ Sci Water Res Technol.* 2019;5:977–992.
- [34] Manz W, Wendt-Potthoff K, Neu T, et al. Phylogenetic composition, spatial structure, and dynamics of lotic bacterial biofilms investigated by fluorescent *in situ* hybridization and confocal laser scanning microscopy. *Microb Ecol.* 1999;37:225–237.
- [35] Burns R, Stach J. Microbial ecology of soil biofilms: substrate bioavailability, bioremediation and complexity. *Dev Soil Sci.* 2002;28:17–42.
- [36] Bitton G. Wastewater microbiology. Hoboken (NJ): John Wiley & Sons; 2005.
- [37] Simoes M, Cleto S, Pereira MO, et al. Influence of biofilm composition on the resistance to detachment. *Water Sci Technol.* 2007;55:473–480.
- [38] Nanda S, Sahu S, Abraham J. Studies on the biodegradation of natural and synthetic polyethylene by *Pseudomonas* spp. *J Appl Sci Environ Manag.* 2010;14:57–60.